Rev. Adv. Mater. Sci. 32 (2012) 68-74

FIBRILLAR γ-ALUMINA POROUS BODY PREPARED BY SLIP CASTING

A. Zamorategui[1], S. Sugita[1], S.Tanaka[2] and K. Uematsu[2]

[1]Department of Chemistry, University of Guanajuato, Guanajuato, Gto., Mexico
[2]Department of Materials Science and Technology, Nagaoka University of Technology
1603-1Kamitomioka, Nagaoka, 940-2188, Japan

Received: July 03, 2012

Abstract. The effects of pH and the concentration of the nano fibers of γ-alumina on the relative density of porous material have been investigated. The viscosity of the aqueous suspensions were determined under controlled rate conditions, varying the pH and solid concentration. It was found that the maximum solid loading in the suspension at pH 4 and 4.5 was 40 and 35 wt.% respectively, and the isoelectric point (IEP) of the powder in the suspension occurs at pH 8.5. The pH values used below the IEP and the resulting agglomeration of the particles affect the relative viscosity of the suspension, and consequently the final relative density of the slip cast body, which at a low pH was higher than that obtained close to the IEP.

1. INTRODUCTION

Porous materials have a network structure with channels and cages that are required in many industrial applications such as electronic sensors, catalysts, high-temperature thermal insulation, filters, biomaterials, etc. Al_2O_3, ZrO_2, TiO_2, and SiO_2 are the most promising candidates due to their thermal and chemical properties. Ceramic materials designed for each specific application require controlling some factors that affect their properties, such as the initial particle morphology and processing technique, including heat treatment. Some of these techniques are partial sintering, direct-foaming, replicating, and removing the template. Partial sintering is a simple processing route for manufacturing porous ceramics starting from porous powder compacts. The fabrication of green compact bodies is achieved by stacking the particles using aqueous slip cast, evaluating certain parameters (ζ-potential, viscosity and solid loading) [1-4]. The fluidity and stability of a colloidal suspension depends on its ζ-potential which is determined by the nature of the suspension such as the type of particles, suspension formulation and pH.

It is well-known that the properties achieved in the final products strongly depend on the morphology of the powders employed [5]. So, in order to improve ceramic quality, it is crucial to evaluate the characteristics of the starting materials and their behavior during processing. They should comprise a calibrated powder or paste with convenient rheological properties which depend on pH, particle size, particle morphology and solid content [6,7]. Colloidal suspensions are commonly analyzed by rheological techniques which are also used as quality control standards that attempt to minimize the variation in suspensions prior to performing the consolidation procedure, i.e. slip cast, so as to control and optimize the microstructure of the final ceramic [8,9]. Thus, the suspension requires a source containing the highest particle content and lowest viscosity possible, which can be related to a high particle mobility and consequently its ζ-potential. As it is known, alumina tends to be positively

Corresponding author: A. Zamorategui, e-mail: zamorategui@ugto.mx

charged at low pH values and negatively charged at high pH values [10,11]. As described by Sugita *et al.* [12], homogeneous precipitation is a suitable method for obtaining fibrillar **-**alumina, consisting of agglomerates with a narrow particle size distribution [13-15]. In the γ-phase, alumina possesses a large surface area, high pore volume, and great catalytic properties which strongly depend on its crystalline structure [16-18]. The purpose of this study is to prepare porous bodies with fibrillar γ**-**alumina obtained by homogeneous precipitation, evaluating the maximum solid loading, viscosity and the agglomerate size varying the pH of the suspensions.

2. EXPERIMENTAL PROCEDURE

Gamma alumina was prepared in the laboratory following the methodology of homogeneous precipitation as described by Sugita *et al.*: spherical submicron particles of basic aluminum sulfate (BAS) are synthesized from a mixture of aluminum sulfate and ammonium bisulfite solutions. This BAS is then neutralized in a solid/liquid reaction with an ammonia solution in order to transform it to aluminum hydroxides. Then, the hydroxides are oven dried at 110 °C to obtain pseudoboehmite (AlOOH) which is in turn used as γ-alumina precursor since it transforms to this phase at 450 °C [19-21].

The morphology and size of the powders were examined by transmission electron microscopy (TEM; Phillips Tecnai F-20 field emission microscope) and a specific surface area was measured for the g-alumina (determined by single-point BET measurements (ASAP 2010 Micromeritrics Instrument Corp., USA,). X-ray diffractometry was used to determine the purity of the phase using CuKα radiation (XRD, MO3XHF22; Mac Science Ltd., Japan). The variation on ζ-potential and the average diameter of the agglomerates were measured using a 10 mM solution of KCl by the electroacoustic technique with a particle size analyzer (AcoustoSizer II, ESA; Colloidal Dynamics, USA).

Dispersions of γ-alumina were prepared using 10, 15, 20, 25, 30, and 35 wt.% of solid content with a milling medium of 90 g of 2-mm zirconia beads introduced into an attrition mill. Hydrochloric acid and ammonium hydroxide were added to adjust the pH (from 4 to 10), milling for 6 h. The viscosity of the suspensions was evaluated using a standard concentric cylinder rheometer (Physica MCR 300 Anton Paar) at 25 °C. Then, the samples were slip cast in 25 mm diameter cylindrical rubber molds, allowing the green bodies obtained to dry under atmospheric conditions and 100 °C. The dried specimens were heated at temperatures of 400, 600, 900, and 1250 °C. The apparent densities of the green bodies were determined by the mass-volume measurement technique and the apparent densities of the heat-treated bodies were measured by the Archimedes method. Thus, the relative densities of the specimens were calculated considering the following real densities: 3, 3.37, and 3.98 g cm^{-3} for the gamma, theta, and alpha alumina phases, respectively. A scanning electron microscope (SEM) (JEOL JSM-6400) was used to observe the morphology on the surface of the bodies.

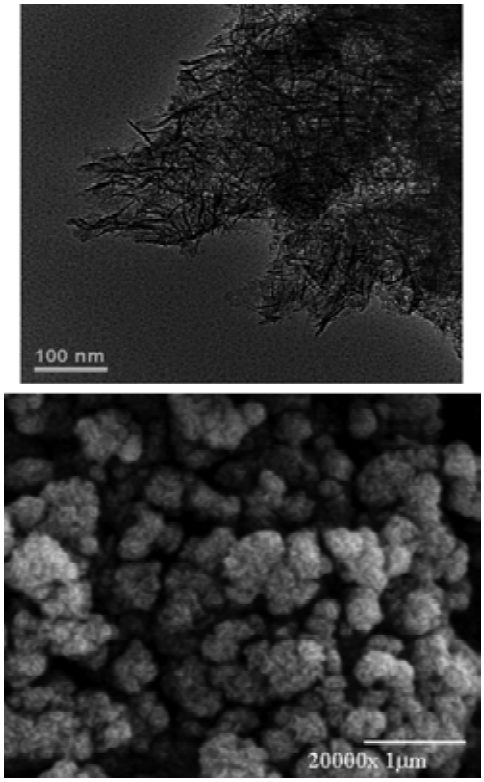

Fig. 1. TEM and SEM images of powder γ-A_2O_3.

3. RESULTS AND DISCUSSION

3.1. Powder characterization

γ-A_2O_3 prepared by homogeneous precipitation consists of nano fibers as shown in Fig. 1a. The TEM image suggests that the fibers have a dimension of 75 nm in length and 3 nm in diameter (aspect ratio of 25), which concurs with the result obtained by BET specific surface area of 334 m^2g^{-1}. On the other hand, the surface morphology observed by SEM (Fig. 1b) shows that the nanofibers tend to form spheroidal agglomerates due to their high surface energy [22].

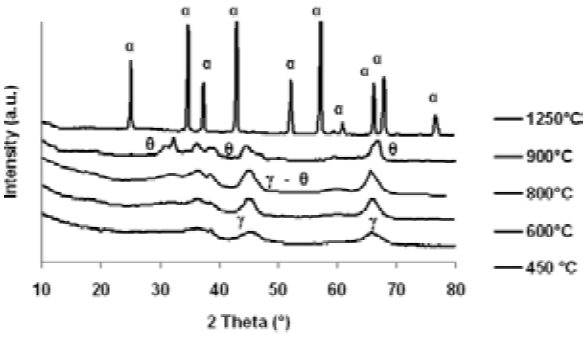

Fig. 2. X-Ray Diffraction of γ-Al_2O_3 sample heated in a temperature range from 450 – 1250 °C: γ, θ, and α mean gamma, theta, and alpha phases of alumina, respectively.

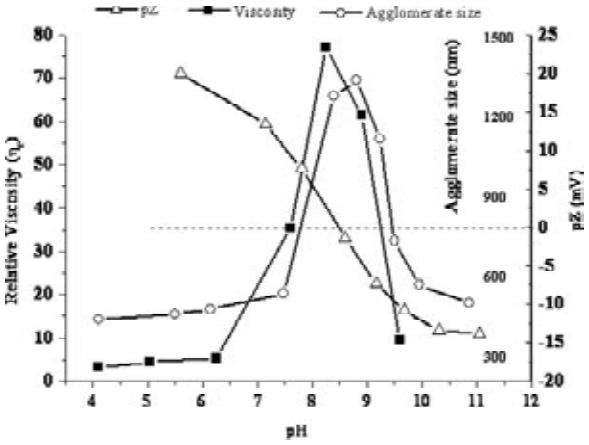

Fig. 3. Apparent viscosity of the 15 wt.% suspension at a shear rate of 200 s^{-1}, agglomerate size and ζ-potential profiles for γ-Al_2O_3 as a function of pH.

Powder X-Ray diffractometry was used to evaluate the crytalline phase evolution of the γ-A_2O_3 obtained in this study (Fig. 2). The evolution of phases was studied in a temperature range from 450 to 1250 °C. XRD of the sample heated at 450°C coincides perfectly with the pattern of γ-A_2O_3 reported (JCPDS No. 10-0425). The sample calcined at 600°C contains a small amount of theta alumina (θ-A_2O_3). As the temperature increases, the signals corresponding to θ-A_2O_3 and the sample at 900 °C shows almost single theta alumina. Finally, the sample heated to 1250 °C contains only alpha alumina (α-A_2O_3).

3.2. Rheological characterization

The zeta potential determination helps to evaluate the stability of suspensions. Fig. 3 shows the effect of pH variation on viscosity, zeta potential and agglomerate size. The profile of the zeta potential vs pH corresponding to changes in surface charge for particles shows the characteristic shape and isoelectric point typical for γ-Al_2O_3. The IEP was found to be at pH 8.5, which is consistent with previously reported data [8,10]. As can be seen, the ζ-potential in the γ-Al_2O_3 suspension is high, either below or above the IEP, i.e., for the particles negatively and positively charged and these changes in ζ-potential are related with the flocculation phenomenon and the rheological behavior of the suspension (Fig. 4a). Thus, below pH 6.3 the agglomerate size remains below 550 nm and has a low viscosity, which is in agreement with the high z-potential measured at these pH values. The agglomerate size and viscosity drastically increase from pH 6.3, reaching their maximum value at about pH 8.5 (IEP) (Fig. 3**),** denoting high flocculation because electrostatic repulsion forces diminish as it becomes comparable to the interparticle van der Waals attractive forces. Finally, the agglomerate size and the viscosity decrease at around pH 9.5 as the particles become increasingly negatively charged generating deflocculation above the IEP, which yields colloidally stable suspensions.

The relative viscosity of a suspension, η_r, is defined as the ratio of the suspension viscosity, h_o, to the solvent viscosity, η_s. Fig. 4b shows the relative viscosity variation of γ-Al_2O_3 suspensions for different solid concentrations, at pH 4 and 4.5. The relative viscosity increases with the solid concentration, and the colloidal suspensions show shear thinning flow behavior at high solid loading (25, 30, and 35 wt.%) and a low shear rate, where the particles maintain a random distribution. But, Newtonian behavior, is achieved at a high sheer rate, indicating that the particle agglomerates in the suspensions were broken with increased shear rate up to 200 s^{-1}, resulting in ordered particle layers.

Fig. 5 shows the relative viscosity of the suspensions as a function of solid content at a shear rate of 200 s^{-1}. At low solid loadings (i.e. up to 15 wt.%) the relative viscosity remains low for both pH's (4 and 4.5). However, the relative viscosity of the suspension starts to increase drastically once solid loading reaches 20 wt.%. Above 35 wt.% the relative viscosity of the suspension at a pH 4.5 rose very sharply, and it does not flow above 40 wt.%. So, the viscosity increases exponentially with the solid loading which corresponds to the curve of fiber suspension flow with a high aspect ratio [23]. For suspensions at a pH 4, the rate of increase is much slower according to its zeta potential. Thus, the

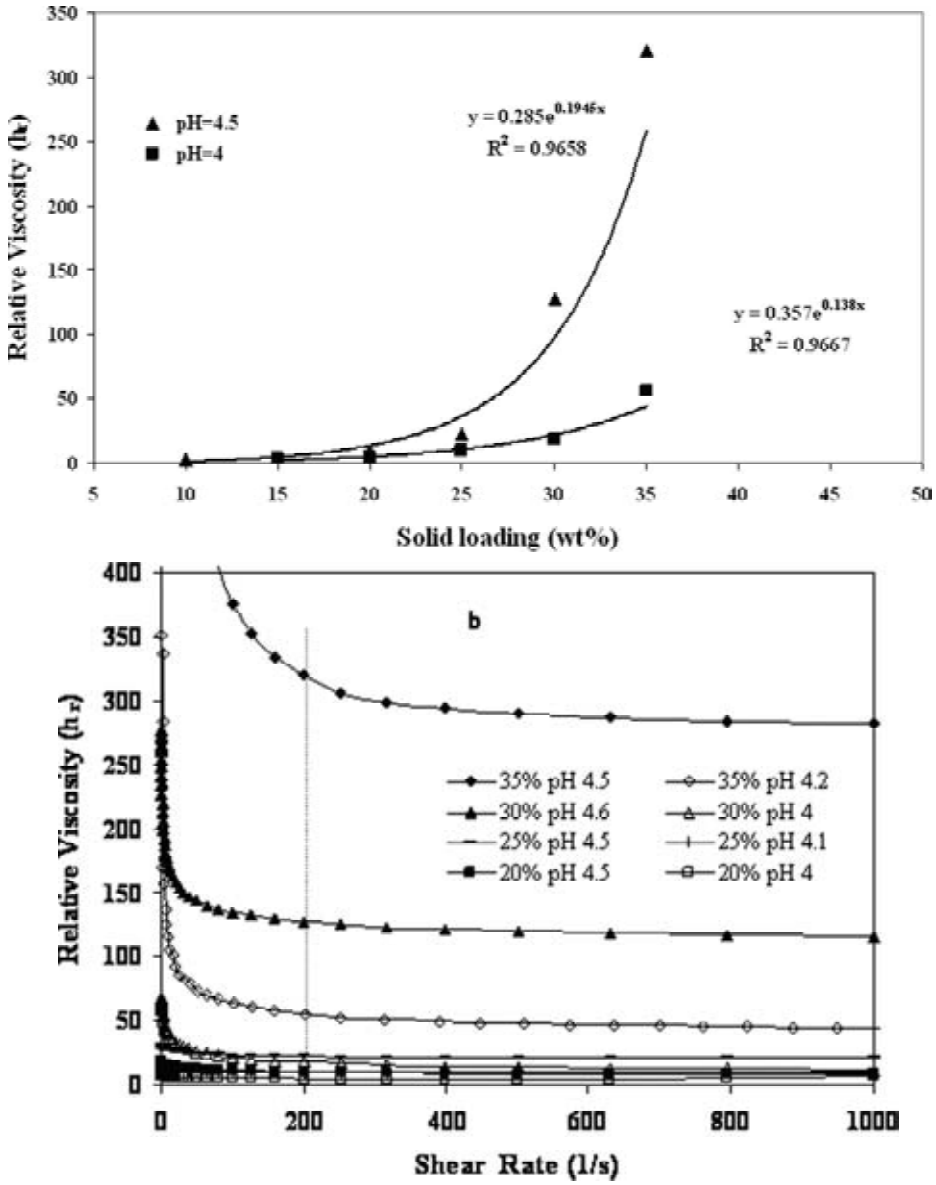

Fig. 4. Relative viscosity versus shear rate of γ-Al_2O_3 suspensions: a) 15 wt.% varying the pH; b) As a function of solid content at pH 4 and 4.5.

particle size, the shape of the particle and pH of the suspension affect its viscosity drastically that can be used to determine the maximum solid loading, which is just enough concentration of the particles that have been added for the viscosity to become infinite.

The viscosity approaches infinity at a maximum solid concentration (ϕ_m) in wt.% at which the average separation distance between the particles tend to zero and the suspension ceases to flow, due to the resistance arising from increased particle to particle contact in the suspension and the particles packed together. The ϕ_m allowable for powder suspension can be predicted following a viscosity solid concentration relationship proposed by the modified Krieger–Dougherty equation [24,25]:

$$\eta_r = \left(1 - \phi / \phi_m\right)^{-n}.$$

As shown in Fig. 6, the ϕ_m at which the suspension behaves as a solid can be estimated by extrapolating the fitted straight line to $(1 - \eta_r^{-1/2}) \rightarrow 1$, obtaining a ϕ_m= 41 and 36 wt.% (Volumetric solid fraction 0.188 and 0.157) at pH 4 and 4.5 respectively. The large difference from the ϕ_m and that of the random close packing (Maximum volumetric solid fraction ~0.64) may provide a measure of the dominant attractive forces, considered important to the porosity reached as a function of pH.

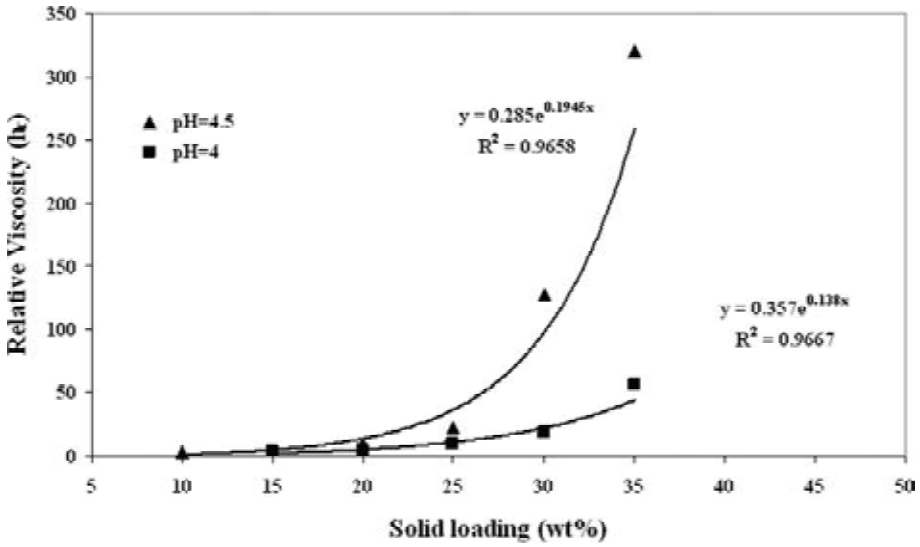

Fig. 5. Relative viscosity at 200 s^{-1} as a function of solid loading at pH 4 and 4.5.

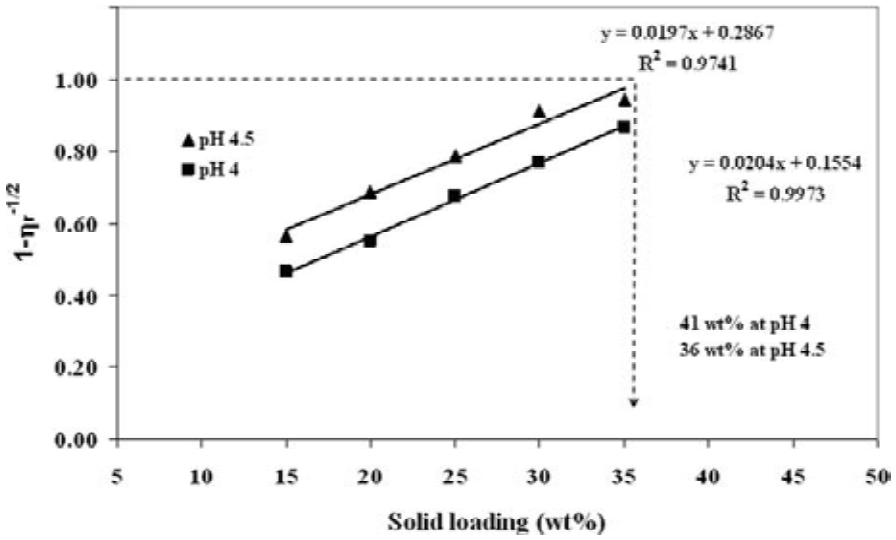

Fig. 6. (1- $\eta_r^{-1/2}$) versus solid loading for γ-Al_2O_3 suspension.

3.3. Porous bodies

Fig. 7 shows the effect of pH on the relative density of the heat treated bodies produced by slip casting. The green bodies from 25, 30, and 35 wt.% suspensions were prepared varying the pH. After heat-treatment at 100, 400, 600, 900, and 1250 °C for 60 min, density was measured. In all cases, the relative density seems to remain constant from 100 to 900 °C and then drastically increases at the high temperature of 1250 °C. This variation can be attributed to the change of phase experienced for γ-alumina which transforms to theta alumina at around 900 °C and finally to alpha alumina at around 1250 °C as shown in Fig. 2. The relative density of the heat treated bodies prepared at pH close to the IEP remains lower than that obtained at a pH far from the IEP. These results are consistent with the observed effect of pH on the viscosity, z-potential and therefore, agglomeration of the powders in the aqueous suspensions. Also, the relative density of heated bodies 25 wt.% was significantly lower than that obtained for 30 and 35 wt.%, which shows the viscosity effects in interparticle contacts. A higher solid loading promotes more particle-particle interactions reducing the interparticle space occupied by water and consequently increases the relative density.

Fig. 8 shows the structural variation observed by SEM of two heat treated bodies (25 and 35 wt.%) at 1250 °C and pH 4. More space between neighboring spheroidal agglomerates for the 25 wt.% body (Fig. 8a) can be observed than that for the 35 wt.% body resulting in a higher compact density as shown in Fig. 8b. Such differences are an effect

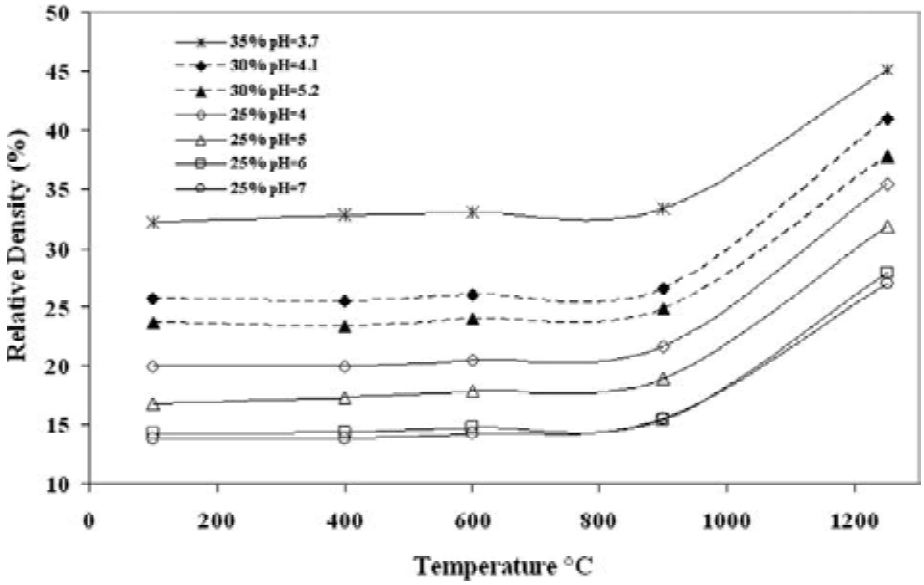

Fig. 7. Relative density of the bodies as a function of heated temperature.

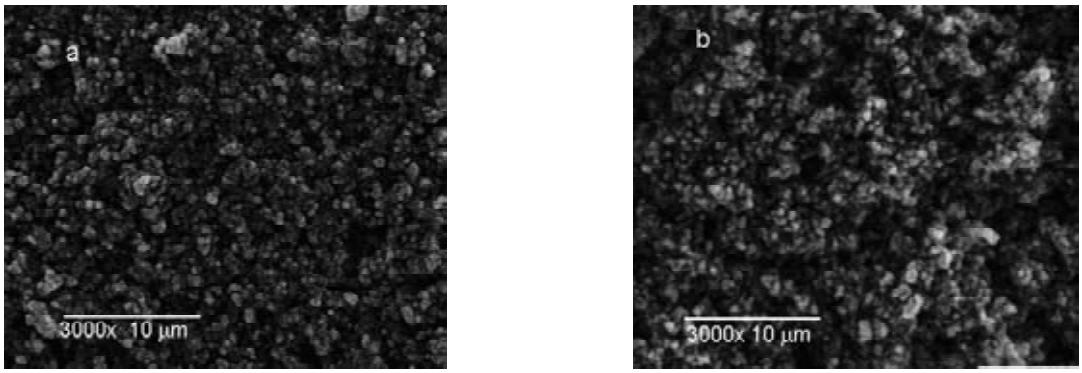

Fig. 8. SEM micrographs of (a) 25 wt.% and (b) 35 wt.% bodies prepared by slip cast at pH 4 and heat treated at 1250 °C.

derived from the solid concentration in agreement with the relative density observed in Fig. 7.

4. CONCLUSIONS

The final densities and porosities of porous compact bodies of fiber γ-alumina were affected by the viscosity, solid loading, and pH of the suspensions. The γ-alumina derived from homogeneous precipitation has a fibrous morphology with a high specific surface area (334 m^2/gr), which makes it necessary to shift to a lower pH in order to obtain Newtonian flow. When the fibrous particles are in suspension there is more energy dissipation which increases the viscosity. Thus, the maximum solid content (41 wt.%) for castable suspension resulted below pH 4.

ACKNOWLEDGEMENTS

We would like to express our gratitude to Nagaoka University of Technology 1603-1Kamitomioka, Nagaoka, Japan 940-2188, for the assistance in the use of the Physica MCR Rheometer.

REFERENCES

[1] F. Tang, H. Fudouzi, T. Uchikoshi and Y. Saca // *Journal of the European Ceramic Society* **24** (2004) 341.
[2] J. F. Yang, G. J. Zhang and T. Ohji // *J. Mater. Res.* **16** (2001) 1916.
[3] A. Kritikaki and A. Tsetsekou // *Journal of the European Ceramic Society* **29** (2009) 1603.
[4] A. R. Studart, U. T. Gonzenbach, E. Tervoort and L. J. Gauckler // *J. Am. Ceram. Soc.* **89** (2006) 1771.
[5] J.K. Beattie and A. Djerdjev // *J. Am. Ceram. Soc.* **83** (2000) 2360.
[6] C. Perego and P. Villa // *Catalysis Today* **34** (1997) 281.
[7] D.J. Kim, H. Kim and J.K. Lee // *Journal of Materials Science* **33** (1998) 2931.

[8] C. Gutiérrez, J. Sánchez-Herencia and R. Moreno // *Bol. Soc. Esp. Ceram.V.* **39** (2000) 105.
[9] E. Behzadfar, M.H. Abdolrasouli, F. Sharif and H. Nazockdast // *Brazilian Journal of Chemical Engineering* **26** (2009) 713.
[10] P. Bowen, C. Carry, D. Luxembourg and H. Hofmann // *Powder Technology*, **157** (2005) 100.
[11] S. Manjula, S. Mahesh Kumar, G.M. Madhu, R. Suresh and M.A. Lourdu Anthony Raj // *Cerâmica* **51** (2005) 121.
[12] S. Sugita, C. Contreras, H. Juárez, A. Aguilera and J. Serrato // *Int. J. Inorg. Mater.* **3** (2001) 625.
[13] R.E. Simpson II, C. Habeger, A. Rabinovich and J.H. Adair // *J. Am. Ceram. Soc*. **81** (1998) 1377.
[14] R. Román, T. Hernández and M. González // *Bol. Soc. Esp. Ceram. V* **47** (2008) 311.
[15] B.K. Park and J.M. Jin // *Journal of Ceramic Processing Research* **9** (2008) 204.
[16] G. Paglia, C.E. Buckley, A.L. Rohl, R.D. Hart, K. Winter, A.J. Studer, B.A. Hunter and J.V. Hanna // *Chem. Mater.* **16** (2004) 220.
[17] F. Tang, T. Uchikoshi, K. Ozawa and Y. Sakka // *Materials Research Bulletin* **37** (2002) 653.
[18] X. Carrier, E. Marceau, J.F. Lambert and M. Che // *Journal of Colloid and Interface Science* **308** (2007) 429.
[19] A.C. Vieira Coelho, G.A. Rocha, P. Souza Santos, H. Souza Santos and P.K. Kiyohara // *Revista Matéria* **13** (2008) 329.
[20] J.R. Viguié, B. Sukmanowski, F. Nölting and X. Royer // *Eng. Aspects* **302** (2007) 269.
[21] S. Kato, H. Unuma, T. Ota and M. Takahashi // *J. Am. Ceram. Soc.* **83** (2000) 986.
[22] A. Zamorategui, S. Sugita, R. Zarraga, S. Tanaka and K. Uematsu // *Journal of the Ceramic Society of Japan* **120** (2012) 290.
[23] D.B. Genovese // *Advances in Colloid and Interface Science* **171–172** (2012) 1.
[24] M.J. Santillán, F. Membrives, N. Quaranta and A.R. Boccaccini // *Journal of Nanoparticle Research* **10** (2008) 787.
[25] P.K. Senapati, B.K. Mishra and A. Parida // *Powder Technology* **197** (2010) 1.